Modelling gene therapy efficiency in mosaic airway organoids for treatment of cystic fibrosis

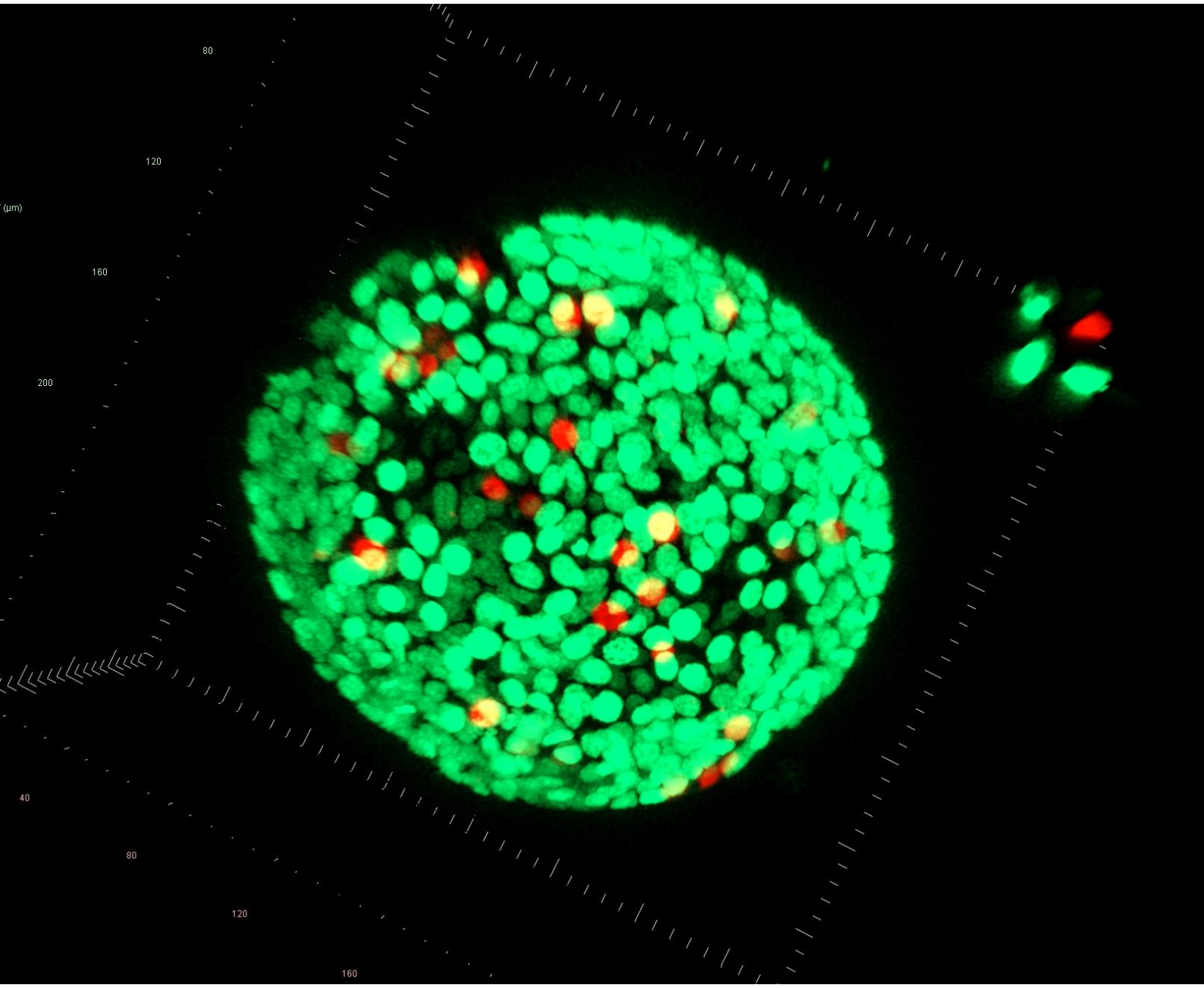

Aileen Griffioen **12/03/25**
Student nr: 6343686
Master student, Regenerative Medicine and Technology

Supervisors: Dr. Ewart Kuijk and Nefeli Ithakisiou
Lab of Cellular Disease Models, RMCU, UMC Utrecht

Abstract

Worldwide over 100,000 people suffer from cystic fibrosis (CF), a recessive genetic disease caused by functional defects of the Cystic Fibrosis Transmembrane Conductance Regulator (CFTR) protein. This disease is characterized by damaging symptoms in multiple organs with respiratory failure as the cause of death for most patients. In the search for treatment options, specific drugs reversing the effects of CFTR mutations at protein level have shown promising results for a number of patients. However, not every type of mutation and therefore not every patient has responded strongly to the currently clinically available drugs, indicating the need for additional treatment options like gene replacement therapy. This treatment option allows for the introduction of a functional copy of *CFTR* into the genome substituting for the loss of CFTR function regardless of the type of underlying mutations. Due to delivery limitations of this treatment option, its use has yet to be translated to *in vivo.* Fortunately, from previous research it is clear that a 100% replacement efficiency is seemingly not necessary for beneficial effects. However, a clear, exact answer to what is required of gene therapy is still missing. Therefore, the aim of this research is determining the number of CFTR-deficient cells required to be effectively treated with gene replacement therapy for total functional recovery of CFTR to relieve or cure patients from their symptoms. This report shows the establishment of an organoid model with differently labelled cells representing CFTR-deficient and -proficient cells and thus gene replacement efficiency. With the use of forskolin-induced swelling of these organoids as an indicator of presence of functional CFTR, in relation to counted cell numbers with computational segmentation, an estimation of the required number of treated cells can be made. For the distinction of functionally different cells within a single organoid, wildtype human nasal epithelial cells (HNECs) were effectively labelled with mNeonGreen or mCherry and can be selected using Fluorescence-activated cell sorting (FACS). Co-cultures of CFTR-proficient mNeonGreen and mCherry labelled cells were differentiated into CFTR-expressing secretory cells and converted into mosaic green and red organoids. To quantify individual cells within these organoids, confocal images were subjected to computational segmentation. To expand this model with incorporation of CFTR-deficient cells, different methods of generating CFTR knockout cell lines were explored, showing potential for future experiments. With further optimization of FACS, incorporation of mutation-specific CFTR-deficient cells, and expansion of computational analysis at low magnification, the organoid model representing gene therapy efficiency can be finalized and used for the estimation of efficiency needed for restoring CFTR function, moving closer to effective and life-changing gene therapy for patients.

Layman summary

Cystic fibrosis (CF) is a disease caused by changes (mutations) in a gene called Cystic Fibrosis Transmembrane Conductance Regulator (*CFTR*). There are numerous of these changes that can cause the disease by preventing correct functioning of the CFTR protein. This interferes with the CFTR-mediated transport of certain particles in multiple organs, like the intestines and lungs. As a result, the concentration of these particles increases in cells, after which water will be attracted to transport from, for example, the airways, into the cells. Because of this, slime in the airways will get less diluted and thicker, eventually damaging the tissue. Primarily damage of lung tissue, significantly lowers the life expectancy of patients.

Treatment with drugs to reverse CFTR dysregulation have shown promising results for some patients, however not all patients have shown a strong response because effects depend on the type of mutations. As research into improvements is still ongoing, another approach, called gene therapy, has been investigated. This approach focusses on introducing a healthy copy of the *CFTR* gene into the DNA to replace non-functional *CFTR*. This method is very promising for all patients because a healthy copy can be introduced regardless of what type of mutation they carry. However, before the approach can be applied, some obstacles need to be overcome. In particular, it is necessary that enough cells receive the healthy copy to reach beneficial effects on lowering symptoms. Gene therapy does not have the capacity to restore CFTR-function in all target cells. However, a lower number of cells with restored function will likely be enough but to determine what this number needs to be and in what way gene therapy can reach this goal, for example in combination with drugs, more research is needed.

Therefore, the aim of this research is to determine the number of cells required to be successfully treated with gene therapy for effective clinical benefits for patients. To work towards this aim, a 3D structure consisting of CFTR-deficient and -proficient cells needs to be established. When present in different ratios, these two cell types represent different ratios of gene therapy efficiency. To distinguish and count these cells to determine the number of healthy versus diseased cells, they were successfully fluorescently labelled by making them produce a fluorescent protein (green or red) that can be visualized under a microscope. By using a specific 3D culture technique, these cells were turned into 3D structures consisting of a combination of both cells in different ratios. Next, these structures can be analysed in specific assays that give an indication of whether healthy CFTR is sufficiently present in the structures or not.

For the future addition of CFTR-deficient cells in the structures, cells acquired from patients can be used or *CFTR* mutations can be intentionally introduced in cells from healthy donors to cause defective CFTR production. In this research, two different methods to introduce these mutations were tested on the airway cells, showing potential for turning off specific genes in these cells.

The successful creation of the 3D structures with differently labelled cells has formed the groundwork of the gene efficiency model. With future incorporation of CFTR-deficient cells, further optimizations of the counting of individual cells and combining this with functional assays, an estimation of the minimal required CFTR-proficient cells for reduction in cystic fibrosis symptoms can be made. This will give insight into how gene therapy can be used for alleviating or curing symptoms of CF patients to get a step closer to an effective treatment.

Introduction

The recessive genetic disease, cystic fibrosis (CF), strongly affects the lives of over 100,000 people worldwide (1–3). Caused by mutations in the Cystic Fibrosis Transmembrane Conductance Regulator (*CFTR)* gene, chloride and sodium exchange between epithelial cells and lumen is dysregulated. As a result, cells experience increased concentrations of these ions and consequently water uptake from the lumen. This eventually leads to thicker mucus, which in turn induces inflammation and increased occurrence of bacterial infections, causing damage to different organs, including pancreas, intestine, and lungs (1).

Over 2000 CFTR mutations, affecting this ion channel, have been identified, with some more prevalent than others (1,2). Their effects on CFTR function differ and can occur at various levels of CFTR expression. To treat these adverse effects and prevent patients' decreased life expectancy primarily caused by damage in the respiratory system, treatment options have been developed for restoring transport function of CFTR (1–3) by reversing mutation-specific defects with so-called modulators. For instance, modulators to improve protein folding or to stimulate channel activation have been shown to be effective. However, not all patients strongly respond to known combinations of modulators as research is still ongoing to improve effectiveness (1). Furthermore, as research is still ongoing, there is yet to be a combination of modulators available for every type of mutation and thus patient (4).

As these modulators target the disease by reversing the effects of *CFTR* mutations at protein level, another approach even further upstream, called gene therapy, holds great potential for every patient regardless of what type of mutations they carry; by incorporating a functional *CFTR* copy into the genome, dysfunctional CFTR can be replaced (4,5). As gene therapy faces challenges in medical practice due to delivery limitations (6), restoring CFTR-function in all targeted cells and thus a 100% efficiency is not possible. However, based on prior research, a lower efficiency would already be sufficient for beneficial effects. That being said, these studies have not represented *in vivo* circumstances well and a consensus about the exact required efficiency has not been reached as their conclusions on efficiency range from 6% to 60%, leaving to wonder exactly how many cells need to be treated with gene therapy (7–13). Additionally, the required efficiency may vary depending on the mutation-dependent reduction of CFTR-activity in diseased cells, as not all mutations lead to full loss of activity (14).

In other words, the question of what level of gene therapy efficiency is needed to restore CFTR function in enough cells to relieve or cure patients from their symptoms dependent on their type of mutation, has yet to be answered. Therefore, the aim of this research is to determine the number of CFTR-deficient cells required to be effectively treated with gene replacement therapy for total functional recovery of CFTR to relieve or cure patients from their symptoms.

CFTR is most abundantly expressed in ionocytes, however as their presence in airway epithelium is very low, the biggest role in CFTR-mediated transport is executed by secretory cells (15). To acquire these cells for research, human nasal epithelial cells (HNECs) can be differentiated using an Air-Liquid Interface (ALI) culture system. In this system, differentiation can be accomplished with the use of a semi-permeable membrane exposing the apical cell surface to air and the basolateral surface to medium (16,17). This way nasal epithelial cells have been used to study various airway diseases, including CF, as these epithelial cells can be donated by patients in a relatively non-invasive manner (18). Following differentiation, the cell monolayer can be fragmented and converted into organoids (19,20).

For functional analysis of these organoids, they can be subjected to Forskolin-Induced Swelling (FIS) assays (17), which utilizes the CFTR-activating effect of forskolin to validate correct functioning of CFTR.

If the number of cells with functional CFTR is sufficient, organoids swell as a result of water uptake. Based on this principle, FIS assays have been used to study potential treatments for CF (21,22).

With the use of these methods, a co-culture of CFTR-proficient and -deficient cells can be differentiated and converted into organoids to establish a gene therapy efficiency model with different ratios of these functionally different cells. For distinction of these cells within the model and enabling them to be counted, the use of lentiviral delivery of H2B-mNeonGreen or H2B-mCherry-expressing vectors combined with confocal imaging and computational processing can be used. With addition of FIS assay analysis, the effect of presence of CFTR-proficient cells on overall CFTR function can be estimated. Utilizing this, this report shows the successful establishment of a green and red mosaic airway organoid model as foundation for and proof-of-concept of a gene therapy efficiency model. Additionally, two methods of knockout generation were explored for the future addition of CFTR-deficient cells to complete the model for gaining more insight into the required number of CFTR-deficient cells corrected with gene editing.

Methods

Cell culture

HEK293

HEK293 cells were cultured for third-generation lentivirus production and as control specific assays. They were passaged (1:10) twice a week and maintained in DMEM (1X) + GlutaMAX (Gibco) (+10% FBS (Sigma, Cat. F7534-500mL) +1% pen/strep (Gibco, REF15070-063)).

HNEC

hTERT immortalized HNECs from one donor and primary HNECs from two donors were cultured as previously described with some adjustments (19). Cells were cultured in FAIR L1 medium (50% Bronchial Epithelial Cell Medium (ScienCell Research Laboratories, Cat. 3211), 44% Advanced DMEM F12 (Gibco, REF12634-010), 2% B27 (Gibco, REF17504-001), 1X pen/strep (Gibco, REF15070-063), 100 µg/mL primocin (Invitrogen, REF ant-pm-2), 0.5 µg/mL hydrocortisone (Sigma, REF H0888), 10 mM HEPES (Gibco, REF15630080), 1.25 mM N-Acetyl-L-cysteine (Sigma, REF A9165-25G), 0.5 µg/mL Epinephrine hydrochloride (Sigma, REF E4642), 5 µM Y-27632 (Selleck Chemicals, REF S1049), 1X GlutaMAX (Gibco, REF35050-061), 1 µM A83-01 (Tocris Bioscience, REF2939/10), 25 ng/mL HGF (Peprotech, REF100-39H), 5 µM DAPT (Fisher Scientific, REF15467109), 100 ng/mL FGF10 (Peprotech, REF100-26_1mg), 2% RSPO3 (ImmunoPrecise, REF R001-100 ml), 50 nM rapamycin (Sigma, REF553210-1 MG), 5 nM Human Heregulin-β1 (Peprotech, REF100-03-100uG)). Cells were passaged approximately once every week at full confluency.

For passaging, culture plates were coated with a collagen IV coating (50 µg/mL in PBS0) (Sigma, REF C7521-10MG). Next, cells were harvested with TrypLE Express Enzyme (Fisher Scientific, REF12605-028) after a PBS0 wash. In Advanced DMEM/F12 they were spun down at 400 g and 4 °C for 5 minutes. The resulting pellet was resuspended in FAIR L1 medium, and cells were counted with an automated Celldrop BF Brightfield cell counter (DeNovix) and passaged based on the following densities: 50,000 cells in a 96-well plate, 100,000 cells in a 24-well plate. 200,000 cells in a 12-well plate, and 500,000 cells in a 6-well plate.

Lentiviral plasmid cloning

DNA vector preparation

A pLV-EF1a-H2B-mCherry-IRES-Blast and a pLV-EF1a-H2B-mNeongreeni-IRES-Blast plasmid were kindly gifted by Martijn Vromans for the introduction of H2B-mNeonGreen or H2B-mCherry into cells alongside a blasticidin resistance gene.

To generate a CFTR-knockout cell line, a lentiviral plasmid carrying the CRISPR/Cas9 system was created by incorporating a gRNA sequence (GCGCCCGAGAGACCATGCAG) (IDT) targeting exon 1, into the lentiCRISPR v2 plasmid with a puromycin resistance gene (Addgene, Plasmid #52961, Gift from Feng Zhang (23)), following the CRISPR Genome Engineering Toolbox from the Zhang lab (24,25) with additional adjustments. To allow for ligation, pre-dimerized gRNA oligos were phosphorylated by adding 2 µL of the dimer to 1 µL of 10X T4 ligase buffer (New England BioLabs, B0202A), 6.5 µL milliQ, and 0.5 µL T4 polynucleotide kinase buffer (10X) (New England BioLabs, B02015). This solution was incubated at 37 °C for 45 minutes and subsequently at 65 °C for 20 minutes.

For digestion of the plasmids, the Restriction Enzyme Digestion protocol (NEBcloner tool, New England BioLabs) (26) was followed by adding 2 µg to 42 µL of nuclease-free water (IDT, 0.2 µm filtered), 5 µL of 10X NEBuffer r3.1 (New England BioLabs, Cat. B7203S), and 1 µL BsmBI (New England BioLabs, Cat. R0580S). Incubation was done at 37 °C for 30 minutes and subsequently at 55 °C for 15 minutes.

To validate plasmid digestion and to isolate correctly digested ones, gel electrophoresis was performed. 1 g of agarose (Eurogentec, REF EP-0010-05) was dissolved in 100 mL of 1X TAE buffer in a microwave for 1 – 2 minutes at max power. When fully dissolved, 5 of SYBR safe DNA gel stain (Invitrogen, REFS33102) was added. Next, the gel was casted in a tray with comb to fully solidify after around 30 minutes. The tray with solidified gel was transferred to an electrophoresis system filled with 1X TAE buffer and approximately 55 µL of digested sample was loaded alongside 10 µL of a GeneRuler 1kb DNA ladder (Thermo Scientific, Cat. SM0311). The gel was run at 125 V for approximately 45 minutes, after which the bands of sizes corresponding with correct digestion were cut out.

Using a QIAquick Gel Extraction kit (Qiagen, REF28706), digested plasmid DNA was extracted from the bands following the manufacturer's procedure. Next, a Qubit dsDNA HS assay kit (Invitrogen, REF Q32854) was used to measure the DNA concentration following the provided procedure.

Ligation of the digested plasmids with the phosphorylated gRNA sequence was performed according to the CRISPR Genome Engineering Toolbox from the Zhang lab (24,25), with some adjustments. 2 µL of 10X T4 Ligase buffer (New England BioLabs, B0202A), 10 µL (20.4 ng) of extracted plasmid DNA, 1 µL of diluted phosphorylated gRNA (1:200 in milliQ), 7 µL nuclease-free water (IDT, 0.2 µm filtered), and 1 µL of a 10X T4 DNA ligase (New England BioLabs) was mixed and incubated overnight at room temperature.

Bacterial transformation

To clone the H2B-mNeonGreen-, H2B-mCherry-, and CRISPR-expressing plasmids, One Shot™ Stbl3™ Chemically Competent E. coli cells (Invitrogen, Cat. C737303) were transformed following the manufacturer's protocol. In short, 1 µL of the pLV-EF1a-H2B-mCherry-IRES-Blast or the pLV-EF1a-H2B-mNeongreeni-IRES-Blast plasmid, or 2.5 µL of the ligation product was added to 17 or 25 µL of Stbl3 cell suspension. The suspension was incubated for 30 minutes on ice and subsequently heated for 45 seconds at 42 °C. After a 2-minute incubation on ice, pre-warmed S.O.C. medium was added up to a total volume of 250 µL. In a shaking incubator, the suspension was incubated for ah hour at 200 rpm and 37 °C. After centrifugation of 2 minutes at 1000 rcf, 200 µL supernatant was discarded and the pellet, resuspended in the remaining 50 µL was spread evenly onto an LA AMP agar plate. The plates were incubated upside down at 37 °C and the following day, single colonies were isolated and added to a 50 mL lysogeny broth with ampicillin (1:1000).

Vector isolation

After overnight incubation in a shaking incubator at 200 rpm and 37 °C, the cell suspension was spun down for 10 - 15 minutes at 3202 rcf. Using a PureLink^{TM} HiPure Plasmid Midiprep kit (Invitrogen, REF K210005), the cell pellets were processed following the provided protocol to isolate the vectors from the selected colonies. Adjustments were made for the centrifugation steps with 30 minutes instead of 10 minutes, 45 minutes instead of 30 minutes and 10 minutes instead of 5 minutes, all at 3202 rcf. The last centrifugation step was repeated before the pellet was air-dried for 5 approximately 5 minutes at 46 °C.

With a spectrophotometer (DeNovix, DS-11) the isolated dsDNA concentration was determined. For future applications, the concentrations were corrected to 1000 ng/µL with TE buffer.

Lentivirus production

For calcium phosphate transfection based on previously reported procedures (27), a 2x HEPES-buffered saline (HBS) solution was prepared. HEPES (50 mM), Na_2HPO_4 (1.5 mM), NaCl (280 mM), KCl (10 mM),

and sucrose (12 mM) were dissolved in 900 mL milliQ on a magnetic rotator. The pH of four equal aliquots of the solution was adjusted to 7.07, 7.09, 7.11, or 7.13, using NaOH. A 2 M $CaCl_2$ stock solution was prepared with 7.35 g in 50 mL milliQ and diluted eight times till 250 mM prior to use.

HEK293 cells were plated on a 10 cm culture dish (100,000 cells/cm^2). The next day, 500 µL of the $CaCl_2$ dilution was added to FACS tubes. Third generation packaging plasmid pRSV-Rev (2.5 µg) (Addgene, Plasmid #12253), envelope plasmid pMD2.G (2.5 µg) (Addgene, Plasmid #12259), and packaging plasmid pMDLg/pRRE (5.0 µg) (Addgene, Plasmid #12251) were added. The plasmids were a gift from Didier Trono (28). Additionally, a transfer plasmid (5.0 g) expressing mNeonGreen, mCherry, or lenti CRISPR/Cas9 was added to create third-generation mNeonGreen-, mCherry- or CRISPR/Cas9-expressing lentiviral particles. Next, 500 µL of 2x HBS (pH 7.11) was added drop by drop while gently vortexing the FACS tube. The resulting solution was evenly added in the medium on HEK293 cells drop by drop.

To produce particles with integrase-deficient vectors for transient expression of CRISPR/Cas9, the pMDLg/pRRE plasmid (Addgene, Plasmid #12251) was replaced by a pMDLg/pRRE plasmid with an inactive integrase gene.

Medium was refreshed on the second day and two taps of virus particles were harvested on the third and fourth day after transfection. For collection, the medium was filtered through a 0.45 µm filter and mixed manually with PEG-based concentrator solution (1/3 of total medium volume) for 1 minute. The solution was incubated overnight at 4 °C on a roller shaker (IKA roller 6) for precipitation of the lentiviral particles.

The next day, the solution was spun down at 1600 rcf and 4 °C for an hour. Polybrene (4 mg/mL) was diluted (1:1000) in 500 µL FAIR L1 medium and added to the virus pellet to enhance transduction efficiency.

Lentiviral transduction

mNeonGreen and mCherry

Immortalized and primary HNECs were transduced with mNeonGreen or mCherry lentivirus alongside HEK293 cells as control. Polybrene (4 µg/mL) was added to the FAIR L1 culture medium. The following transduction assays were performed:

Table 1: Lentiviral transduction conditions for immortalized and primary Human Nasal Epithelial Cells. The percentage of virus is the percentage of the total volume of produced virus in 500 µL culture medium. The time of transduction is the day the transduction was started after plating of the cells with day 0 being the day of plating.

Cell type	Plate type	Cell density (cells/well)	Virus (%)	Time of transduction
Immortalized	96-wells	50,000	40, 20 and 10	Day 7
Primary	12-wells	300,000	20	Day 0

Cells were passaged approximately once a week when at full confluency.

CRISPR/Cas9

Transduction with CRISPR/Cas9 (integrating or non-integrating) was performed on immortalized HNECs positive for mCherry. 100 µL of each virus was added to 500,000 cells seeded in a 12-well plate with 1 µL polybrene (4 µg/mL). A control of mNeonGreen-positive cells was used to validate proper culture conditions, and an mNeonGreen control for puromycin selection without prior transduction to validate

puromycin-induced cell death. Cells were passaged around once a week when at full confluency and maintained in FAIR L1 medium.

Positive selection

Blasticidin

Immortalized mNeonGreen- and mCherry-positive cells were selected with 8 µg/mL blasticidin for three days unless stated otherwise.

To determine the optimal blasticidin concentration for future positive selection of labelled cells, immortalized HNECs were subjecting to a dilution range (0, 0.5, 1, 2, 4, 5, 8, 10, 16, 20, 40, and 80 µg/mL) of blasticidin (InvivoGen, Cat. ant-bl-05) in FAIR L1 medium. 50,000 or 10,000 cells were plated and blasticidin was added after 3 or 4 days, respectively. As readout, brightfield images were taken every day to analyse cell death.

Puromycin

The cells transduced with CRISPR/Cas9 and control cells were selected with 1 µg/mL puromycin following an overnight (16-17 hours) transduction.

Fluorescence-activated cell sorting (FACS)

Primary cells were not positively selected with blasticidin, but were sorted with FACS to investigate usability of FACS. Approximately 3 x 10^6 mNeonGreen- and mCherry-positive primary HNECs were harvested and spun down at 400 g and 4 °C for 5 minutes. Pellets were resuspended in 500 µL FACS buffer (5% FBS (Sigma, Cat. F7534), 1:200 EDTA, 10 µM Y-27632) and filtered through a FACS tube strainer cap to eliminate clustering of cells. The cells were then stained with DAPI (2 µg/mL) (Sigma, Cat. D9542) to allow for sorting of viable cells. Next, 100,000 mNeonGreen- and 90,000 mCherry-positive cells selected for fluorescence within a specific range were sorted. After sorting, Advanced DMEM/F12 was added and spun down at 400 g and 4 °C for 5 minutes to remove FACS buffer. Lastly, cells were resuspended in 500 µL FAIR L1 medium and seeded in a 24-well plate coated with collagen IV.

Ribonucleoprotein CRISPR/Cas9

200 µM of tracrRNA (IDT, Cat. 1072533), 100 µM of Hs.Cas9.CFTR.1.AC crRNA (AATCTGTTAAGGCATACTGC) (IDT) targeting exon 7 of CFTR, and 100 µM of FOXJ1 crRNA (GAGAGTCCCCGCAGACATGG) (IDT) was prepared in Duplex Buffer (IDT, 0.2 µm filtered) after which gRNA was formed by mixing tracrRNA and crRNA in Duplex Buffer till 10 µM before heating (till 95 °C) and cooling (room temperature). Alt-R™S.p.Cas9NucleaseV3 (IDT, Cat. 1081058) was diluted in PBS (1:10) and 1 µL was added to 21.78 µL Opti-MEM I Reduced Serum Medium (Gibco, Cat. 31985-047) and 1 µL Cas9 Plus™ Reagent (Invitrogen, REF CMAX00001). Next, 1.22 µL of gRNA was added and incubated for 10 minutes to generate the ribonucleoprotein. 0.75 µL of Lipofectamine CRISPRMAX Transfection Reagent (Invitrogen, REF CMAX00001) was incubated in 24.25 µL Opti-MEM for 7 minutes at room temperature and subsequently with the ribonucleoprotein mix for another 7 minutes.

During the incubation times, immortalized and primary HNECs from different donors were harvested and seeded in a collagen IV coated 24-well plate (50,000/well) in 500 µL FAIR L1 medium. Next, the CFTR and FOXJ1 ribonucleoprotein-lipofectamine solutions were each added to both immortalized and

primary cells for 16 hours before medium was refreshed with FAIR L1 medium. Cells were passaged around once a week based on concluency before being processed for sequencing.

Sanger sequencing

For validation of correct CFTR gRNA ligation into the digested CRISPR/Cas9 vector, Sanger sequencing was performed. A primer against the hU6 promoter (GACTATCATATGCTTACCGT) (IDT) upstream of the incorporated gRNA sequence was diluted (1:10) and 1 µL was added to 9 µL of isolated vector DNA. Sequencing was performed by Macrogen and analysed with the use of Benchling.

Furthermore, sequencing was performed to analyse the effect of the knockout methods. >100,000 cells were centrifuged at 400 g and 4 °C for 5 minutes. gDNA was isolated from the pellets with a Quick-DNA microprep kit (Zymo Research, Cat. D3021) following the provided protocol.

For amplification of the gDNA, 10 µM dilutions of the following primers (ordered from IDT) were prepared in nuclease free water (IDT, 0.2 µm filtered): CFTR exon 1 forward (FW) (AATTGGAAGCAAATGACATC), CFTR exon 1 reverse (RV) (TGAAGAATCATTTACCTGTG), CFTR exon 7 FW (TGAGTCTGTACAGCGTCTGGC), CFTR exon 7 RV (CACCCTGGACCAACTACATAAAAC), FOXJ1 FW (ACATACTTATTCGGAGGAGGCGC), and FOXJ1 RV (TGAACCTGGCACCTGGTGGTAG). For each sample, 5 µL gDNA was added to 11.25 µL nuclease free water (IDT, 0.2 µm filtered), 5 µL GreenGoTaq buffer (Promega, REF M891A), 2 µL $MgCl_2$ (Promega, REF A351H), 0.5 µL dNTP (Promega, REF U151B), 0.25 µL GoTaq G2 flexi DNA polymerase (Promega, REF M780B), 0.5 µL FW primer, and 0.5 µL RV primer.

The following PCR settings were used on a T100 Thermal Cycler (Bio-Rad): Initial denaturation for 2 minutes at 95 °C. 35 cycles of denaturation for 30 seconds at 95 °C, annealing for 60 seconds and extension at 72 °C. The final extension was 5 minutes at 72 °C ending with a 12 °C infinite hold.
The annealing temperature used for the ribonucleoprotein CFTR exon 7 samples, was 60 °C and the extension time was 32 seconds. For the ribonucleoprotein FOXJ1 samples this was 62 °C and 22 seconds and for the lenti CRISPR CFTR exon 1 samples 47 °C and 45 seconds was used.

The PCR product was processed in gel electrophoresis, to check for the absence of aspecific products, following aforementioned procedure with some adjustments; 10 µL SYBR safe DNA gel stain was added. 1 µL of a 100 bp GeneRuler DNA ladder (Thermo Scientific, REF SM0241) was added to 8 µL nuclease free water (IDT, 0.2 µm filtered) and 2 µL loading dye. 5 µL of this solution and 5 µL of sample was loaded into the gel. The gel was run for at least 45 minutes at 100 V (80 V the first 10 minutes) or at 125 V.

For the ribonucleoprotein CRISPR/Cas9 samples, purification of the PCR product was performed using a Gel and PCR clean-up kit (Nucleospin, REF740609.250) according to the manufacturer's procedure.

dsDNA concentration was measured using a spectrophotometer (DeNovix, DS-11). Around 200 - 250 ng of purified PCR product (ribonucleoprotein samples) and unpurified PCR product (lenti CRISPR samples) was added to 1 µL CFTR exon 7 forward primer (TGAGTCTGTACAGCGTCTGGC) (IDT) or 1 µL FOXJ1 forward primer (ACATACTTATTCGGAGGAGGCGC) (IDT) and CFTR exon 1 forward primer (AATTGGAAGCAAATGACATC) (IDT) respectively in nuclease-free water up till 10 µL. Sequencing was performed by Macrogen and analysed with the use of Benchling.

Air-liquid interface differentiation

HNECs were differentiated into secretory cells, as previously reported (19), for the purpose of generating organoids to be analysed based on their CFTR-mediated forskolin-induced swelling. For the differentiation, the apical side of Transwell Permeable Supports 6.5mm inserts (Costar, REF3470) in a 24-well plate were coated with purecol (1:100 in PBS0) (Advanced BioMatrix, Cat. 5005-100mL). After minimally an hour, 200,000 cells (100,000 mNeonGreen + 100,000 mCherry) were seeded with 800 µL FAIR L1 on the basolateral side and 200 µL on the apical side. After three to seven days, at full confluency, medium was replaced with ALI diff medium (492.2 mL Advanced DMEM/F12, 1% v/v pen/strep (Invitrogen), 5 mg/mL Epinephrine (Sigma-Aldrich, E4642), 100 nM TTNPB (Cayman Chemical, 16144-1), 0.5 ng/mL hEGF (Peprotech, AF-100-15), 50 nM A83-01 (Tocris Bioscience, 2939), 100 nM Triiodothyronine (Sigma-Aldrich, T6397), and 0.5 µg/mL hydrocortisone (Sigma-Aldrich, H0888) supplemented with A83-01 (1:10,000). For approximately three days, but max seven days, cell morphology was monitored and once a complete, homogeneous morphological change was observed across the monolayer, the culture was switched to air-exposed with no apical medium and 600 µL ALI diff medium supplemented with A83-01 (Tocris Bioscience) and Human Heregulin-β1 (Peprotech) on the basolateral side. The last transition was done after approximately three to five days, based on morphology, by changing the medium to 600 µL ALI diff medium with Human Heregulin-β1 basolaterally.

Organoid conversion

To convert fragments of the differentiated monolayer into organoids as previously described (19,20), the monolayer was washed with 100 µL Advanced DMEM/F12 and incubated for 5 minutes at 37°C and 5% CO_2. Next, 600 µL of collagenase type II solution (Gibco, REF 17101-015) (1:20 in Advanced DMEM/F12) was added on the basolateral side for 45 minutes at 37 °C and 5% CO_2. With 100 µL Advanced DMEM/F12, the cells were collected and transferred into 1 mL Advanced DMEM/F12. To acquire fragments, the monolayer was disrupted with a P10 or P200 pipette tip on a P1000 tip. The size of the fragments was checked under a microscope till most fragments were of desirable sizes (30 µm – 100 µm). 4 mL of Advanced DMEM/F12 was added to the suspension and strained through a 100 µm strainer (puriSelect, REF43-57100-01) on top of a 30 µm strainer (pluriSelect, REF43-50030-01). The 30 µm strainer was turned upside down and with 5 mL Advanced DMEM/F12 the fragments were washed off the strainer and collected. The suspension was centrifuged at 400 g and 4 °C for 5 minutes after which the pellet was resuspended in 60 µL Matrigel (Corning, Cat. 354230). Droplets were created in a pre-warmed 24-well suspension plate and the plate was incubated at 37 °C and 5% CO_2 for 2 minutes before being turned upside down. After an incubation of 15 – 30 minutes, medium was added (AO2 medium (472.5 mL Advanced DMEM/F12, 1X GlutaMAX (Invitrogen), 50 U/mL pen/strep (Gibco), 10 mM HEPES (Gibco), 2% B27 (Gibco), 1.25 mM N-acetyl-cysteine (Sigma-Aldrich), 5 mM nicotinamide (Sigma-Aldrich), and 500 nM A83-01 (Tocris Bioscience)) supplemented with 10 ng/mL FGF10 (Peprotech), 5 ng/mL FGF7 (Peprotech) and 5 µM DAPT (ThermoFisher Scientific)).

Forskolin-induced swelling assay

Assay

To prepare organoids for FIS assays as previously reported (19,20), they were transferred to an uncoated 8-well µ-Slide (Ibidi, Cat. 80801) or a black 96-well plate (Corning or Greiner) after three to five days. For this, medium was replaced with 400 µL cell recovery solution (Corning, REF354253) to dissolve the Matrigel. The plate was incubated at 4 °C for 20 to 30 minutes and the organoid suspension was collected in 4 mL Advanced DMEM/F12. Next, the organoids were spun down at 400 g for 5 minutes. To determine the needed amount of Matrigel for an ideal organoid density, a 4 µL test droplet was created. If necessary, the density was adjusted and once ideal, the rest of the organoids were plated in 4 µL droplets. The plate was then incubated for 2 minutes at 37 °C and 5% CO_2 before being

flipped and incubated for another 15 to 30 minutes. Finally, 100 µL AO2 medium was added and switched to FIS assay medium (AO2 medium, 0.5 nM neuregulin-1β (Peprotech, REF100-03_100UG), 10 ng/mL interleukin-1β (Peprotech, REF200-01B_10UG) three to ten days before performing the FIS assay.

For the FIS assay, 10 µM of forskolin (Sigma-Aldrich, Cat. F3917) or DMSO (Sigma-Aldrich, Cat. D4540) in Advanced DMEM/F12 was prepared after which, the solutions were added to three or five wells each. Next, the expected swelling in the forskolin groups and a lack thereof in the DMSO control groups was imaged on a Celldiscoverer 7 microscope (ZEISS) during a period of an hour with brightfield images taken every ten minutes.

Analysis

Swelling was analysed with OrgaSegment (29), a deep-learning segmentation model, to calculate a change in total organoid area over time in every well. This was then converted into an area under the curve (AUC) value per well.

Statistical analysis was done with a Student's t-test using GraphPad Prism 10.4.1.

Microscopy

Fluorescence images of mNeonGreen- and mCherry-positive cells were acquired using an EVOS cell imaging system (Life Technologies) with the GFP and RFP channels respectively. For brightfield images of HNECs, a DMi1 inverted microscope (Leica) was used, and organoid imaging was performed with a Celldiscoverer 7 microscope (ZEISS) in brightfield for OrgaSegment analysis and confocal for Deformable Mesh 3D (DM3D) segmentation.

Deformable Mesh 3D (DM3D) segmentation

Segmentation of the mosaic organoids was accomplished by dr. Matthew Smith by analysing confocal images at 10x of 5x magnification using the Deformable Mesh 3D plugin (DM3D) for Fiji and ImageJ (30,31).

Results

Effective nuclear labelling of HNECs via lentiviral transduction

To build the mosaic organoid model, immortalized and primary HNECs from the same donor were subjected to lentiviral transduction of H2B-mNeonGreen- or H2B-mCherry-expressing vectors. This method proved successful in both the primary as immortalized cells (Fig. 1a,d). Transduction efficiency in both was high, with most cells expressing the fluorescent proteins, showing that these cells can be effectively modified using lentiviral transduction. However, surprisingly long-term culture of the mCherry-positive cells, but not the mNeonGreen cells, appeared challenging as there was a noticeable gradual loss of mCherry-positive cells within the culture (Fig. 1b). Although those specific cells were not positively selected, thus negatively labelled cells were expected and observed in both green and red populations, visibly and considerately more loss of mCherry-positive cells was visible. Brightfield imaging showed full confluency and thus presence of unlabelled cells.

For positive selection to eliminate unlabelled cells, a selection method based on blasticidin resistance was explored. Since the mNeonGreen and mCherry vectors carry a blasticidin resistance gene, the cells can be selected with a blasticidin concentration lethal for negatively transduced cells. To determine this concentration, immortalized HNECs were incubated with different concentrations of blasticidin. Results of these blasticidin selection experiments (Fig. 1c), showed visible cell death and morphological changes caused by low blasticidin concentrations (0.5 – 5.0 µg/mL) after three days. Noticeably, in all conditions, not all cells fully detached from the plate, including in the highest concentration condition (80 µ g/mL).

Additionally, an alternative method of selection, with the use of FACS, was tested on primary HNECs (Fig. 1d). The goal of this method was to both eliminate negatively transduced cells and select cells with the same fluorescent intensity for easier microscopic visualization. With this sorting method, a population of cells with a more homogeneous expression of mNeonGreen or mCherry was successfully acquired. However, some negatively transduced cells were still sporadically visible (Fig. 1d).

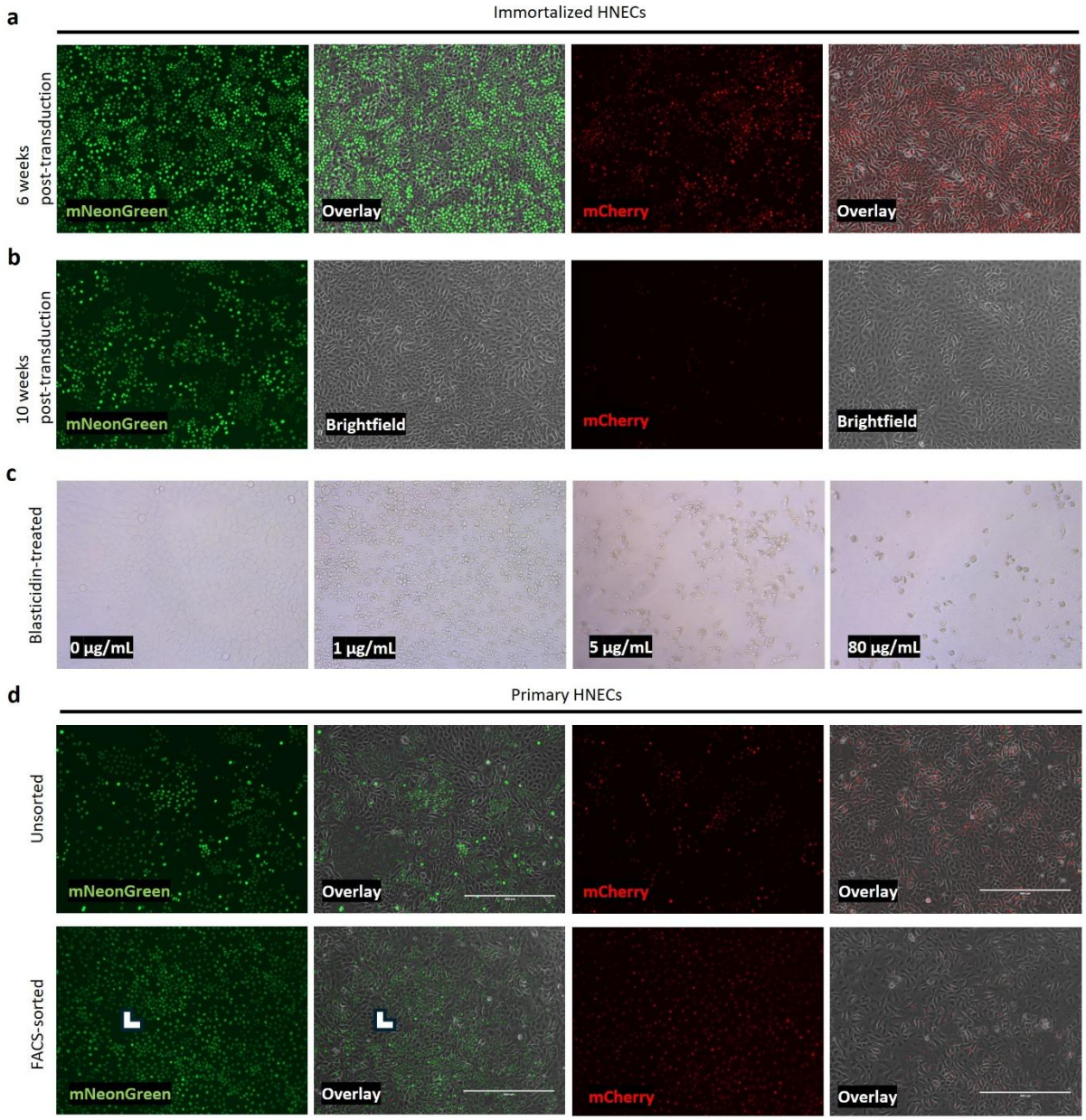

Figure 1: Lentiviral transduction and selection of immortalized or primary Human Nasal Epithelial cells (HNECs) for mNeonGreen or mCherry nuclear labelling. Cells were imaged at 10x magnification. Overlays were created with fluorescence and brightfield images. a) Immortalized HNECs six weeks after transduction with a mNeonGreen- or mCherry-expressing lentiviral vector. Cells were selected with 8 µg/mL for three days. b) Immortalized HNECs ten weeks after transduction with a mNeonGreen- or mCherry-expressing lentiviral vector. Cells were not positively selected. c) Immortalized HNECs treated with different concentrations (1, 5, and 80 µg/mL) of blasticidin for three days, compared to a 0 µg/mL control. d) mNeonGreen- or mCherry-labelled primary HNECs before (unsorted) or after FACS. White arrows indicate negatively labelled cells.

Successful creation of mosaic organoids consisting of labelled HNECs

After the effective labelling of HNECs, their ability to differentiate into CFTR-expressing secretory cells and converted into organoids was investigated. Both cell lines were successfully differentiated and converted into organoids in a mixed condition directly following differentiation (Fig. 2). Confocal imaging showed the evenly distribution of mNeonGreen- and mCherry-positive immortalized HNECs seeded on an ALI transwell insert in a 1:1 ratio (Fig. 2a). The organoids derived from the differentiated mixed condition, showed a combination of green and red cells in individual organoids (Fig. 2b).

Noticeably, the 1:1 ratio the cells were seeded and differentiated in was not reflected in the imaged organoids, showing expected variety in ratios across different individual organoids.

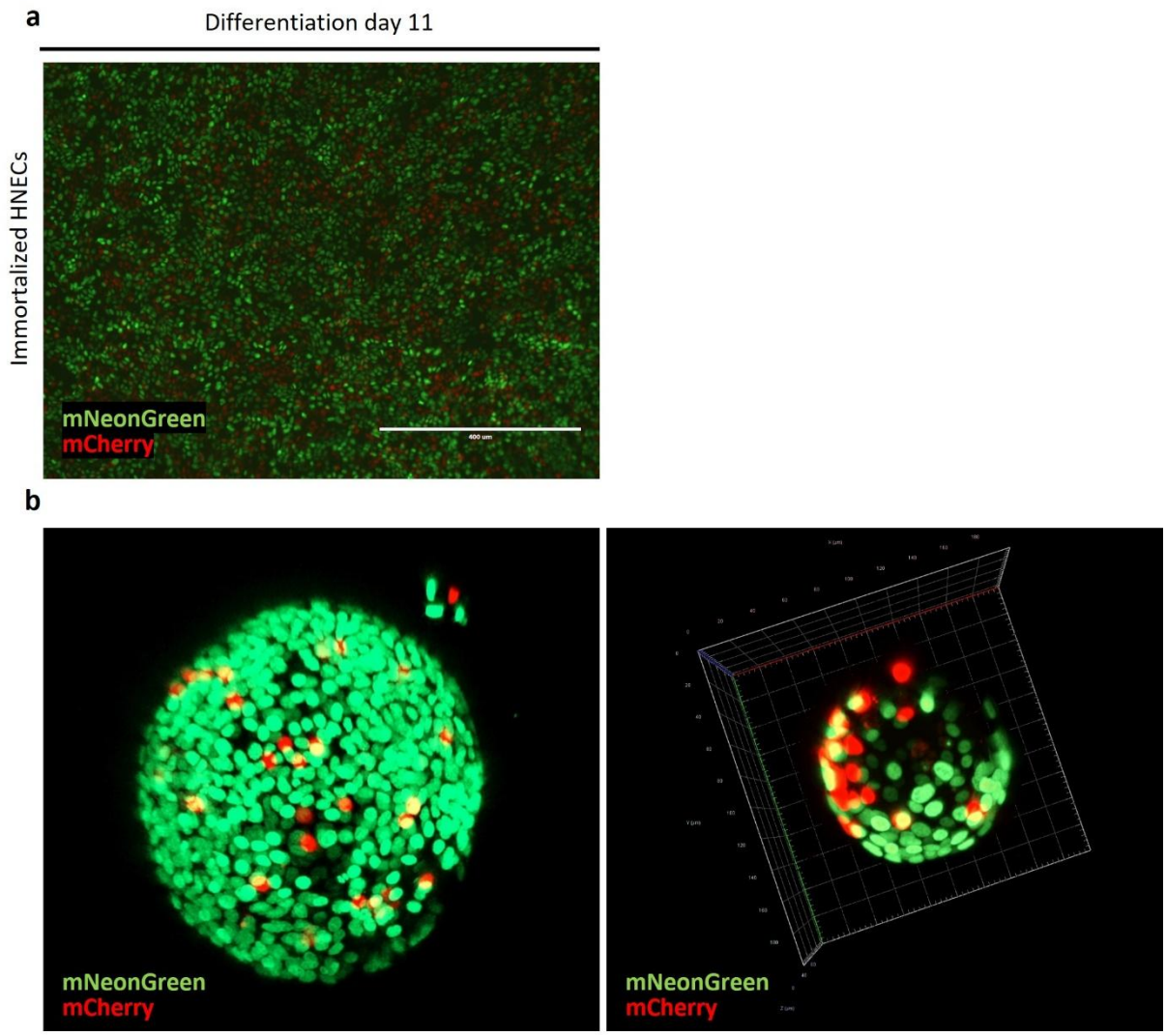

Figure 2: Differentiation and organoid conversion of immortalized Human Nasal Epithelial cells (HNECs) labelled with mNeonGreen or mCherry. a) mNeonGreen and mCherry cells combined on Air-Liquid Interface inserts and differentiated into secretory cells. Imaged at 10x magnification b) Differentiated cells converted into mosaic organoids. Imaged at 10x magnification.

Mosaic organoids show functional swelling and individually labelled nuclei in computational processing

For the assessment of cell ratios in relation to forskolin-induced organoid swelling, mosaic organoids were treated with forskolin (5 µM) for an hour. Brightfield images acquired every ten minutes have subsequently been analysed with OrgaSegment to calculate a total AUC based on change of total organoid area over time. This analysis showed noticeable swelling in the brightfield images (Fig. 3a) and reflected in the AUC of the forskolin condition compared to the 0 µM control condition ($p>0.05$) (Fig. 3b).

By processing the mosaic organoids with Deformable Mesh 3D (DM3D) segmentation, individual green and red nuclei were possible to be recognized in confocal images at 10x magnification (Fig. 3c). To investigate the possibility of replicating this at 5x magnification to enable the processing of a larger

number of organoids at once, confocal images were acquired at 5x magnification (Fig. 3d). This magnification enables individual organoids in the confocal images to be recognized in the corresponding brightfield images analysed with OrgaSegment, allowing for their cell count to be linked to their individual swelling in OrgaSegment. DM3D segmentation of these images showed the need for optimization of confocal imaging regarding laser power and exposure time for correct distinction of individual nuclei. Furthermore, some surprisingly elongated nuclei were visible, suggesting a need for optimizations of the imaging in the z-direction. Finally, the pixel size made a difference in quality of segmentation.

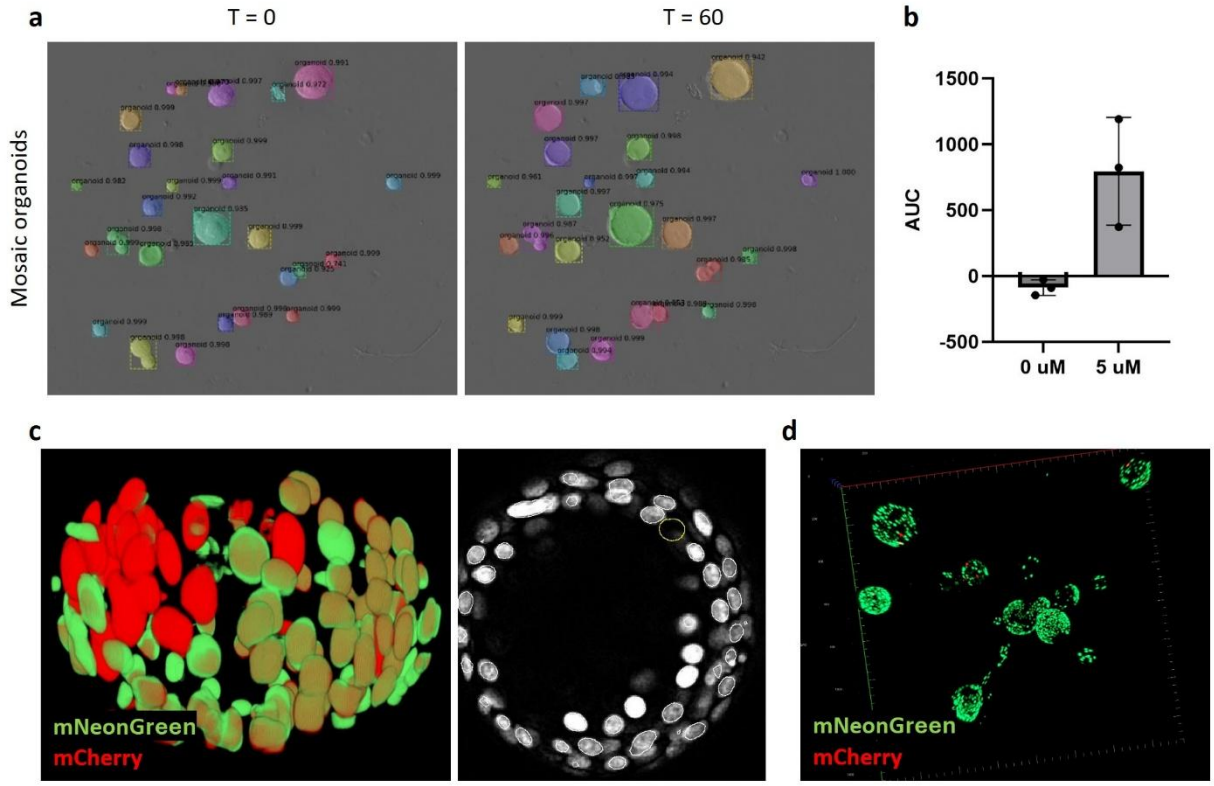

Figure 3: Functional analysis and computational processing of mosaic organoids. a) Forskolin-induced swelling of mosaic organoids after an hour (T=60) of 5 µM forskolin treatment, analysed a) and converted b) into an Area Under the Curve (AUC) value with the use of OrgaSegment. c) Computational segmentation of confocal images of mosaic airway organoids at 10x magnification using the Deformable Mesh 3D plugin (DM3D) in Fiji. d) Confocal imaging of mosaic organoids at 5x magnification. Cells were not positively selected prior to organoid conversion.

Genetic modification methods show potential in generating a CFTR knockout in HNECs

Altogether, the results show the successful labelling and differentiation of cells and the subsequent generation of a mosaic airway organoid model.

Next, to expand the mosaic model with the future addition of CFTR-deficient cells, the possibility of creating a CFTR knockout in HNECs was investigated to expand the model with the use of CFTR-deficient cells. For this purpose, different knockout methods were applied. For one of these methods, a lentiviral vector carrying the CRISPR/Cas9 system and a puromycin resistance gene, was created and introduced to the immortalized mCherry population. For positive selection, two concentrations of puromycin (1 and 2 µg/mL) were assessed. Both conditions showed survival of resistant cells, however, 2 µg/mL caused stress in the resistant cells, preventing further proliferation. Therefore, cells selected with 1 µg/mL (Fig. 4a) were further processed and analysed with Sanger sequencing.

Additionally, transduction of a non-integrating virus for transient CRISPR/Cas9 expression was evaluated with puromycin selection approximately 18 hours post transduction (Fig. 4a). The presence of resistant cells was visible after selection, but not a sufficient amount to sustain a culture.

Results of the sequencing of the lentiviral CRISPR/Cas9 treated cells showed a shift in DNA sequence, starting from the Cas9 cutting site (Fig. 4b), indicative of presence of indels and thus CRISPR/Cas9 activity. Unexpectedly, traces of the wildtype sequence are present despite that the cells were selected for successful transduction with puromycin.

Another method of CRISPR/Cas9 delivery (32), was assessed on immortalized and primary HNECs. As this method has been effectively used to create a FOXJ1 knockout in HBECs (32), FOXJ1 was included in this research as a control alongside CFTR. The method showed a sequence shift in primary HNECs after the Cas9 cutting site, but also before (Fig. 4c) with a sudden sequence shift approximately 91 nucleotides upstream of the cutting site. Furthermore, a careful indication of indels in FOXJ1 in immortalized HNECs was observed but at low efficiency (not shown).

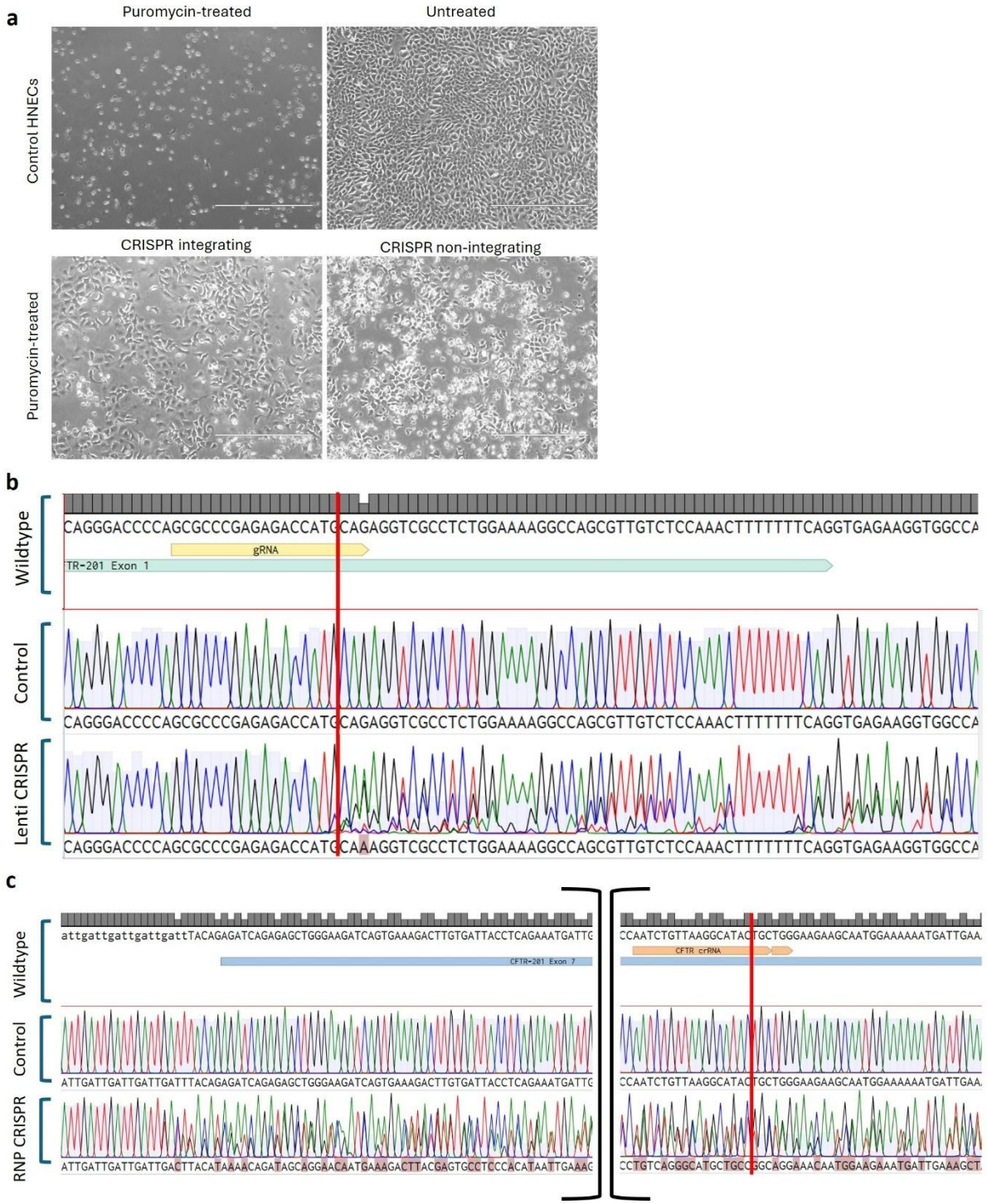

Figure 4: Analysis of Human Nasal Epithelial cells (HNECs) treated with a lentiviral CRISPR/Cas9 (Lenti CRISPR) method or a ribonucleoprotein method (RNP CRISPR). a) Positive selection of immortalized HNECs introduced with a lentiviral CRISPR/Cas9 vector targeting CFTR with or without the ability to integrate into the genome. Cells were transduced with lentivirus for 16-17 hours before selected with 1 µg/mL puromycin. Untransduced cells either untreated or treated with puromycin (1 µg/mL) were used as control. All images were acquired with an EVOS cell imaging system at 10x magnification. b) Sanger sequence results of immortalized mCherry-transduced HNECs treated with additional transduction of integrating lentiviral CRISPR/Cas9 particles targeting CFTR exon 1. Results are displayed with the wildtype sequence compared to untreated control cells and the treated samples. The red line represents the Cas9 cutting site three nucleotides upstream of the PAM sequence. c) Sanger sequence results of primary HNECs treated with a ribonucleoprotein CRISPR/Cas9 lipofection method targeting CFTR exon 7. Brackets indicate part of the sequence left out for displaying purposes.

Discussion

This report shows successful creation of a mosaic airway organoid model for the future assessment of CFTR-recovery in relation to gene therapy efficiency. For the distinction of two functionally different cells in single organoids, lentiviral nuclear labelling of primary and immortalized HNECs was shown to be effective with high transduction efficiencies. The additional use of positive selection based on FACS, creates the potential for acquiring a homogeneous population of mNeonGreen- or mCherry-positive cells with limited variety in microscopic signal intensity.

With further optimization regarding FACS gating to ensure elimination of all unlabelled cells, the model can be created with a mix of solely green and red cells with homogeneous fluorescence intensities. This homogeneity potential of FACS selection makes this method preferable compared to blasticidin selection. However, first some challenges need to be overcome regarding the mCherry cell population. The observed gradual loss of labelled cells suggests an endogenous effect on cell viability caused by the mCherry construct. As this effect was not observed in the mNeonGreen population, it is advised to search for an alternative of mCherry that just like mNeonGreen will not influence cell proliferation.

The established method to label the airway cells, allows for the future incorporation of CFTR-deficient cells. For this purpose and future applications, different methods to generate a CFTR knockout were investigated. Sanger sequencing showed indels created before the Cas9 cutting site in cells treated with CRISPR/Cas9 as ribonucleoprotein. This could mean presence of a large deletion; however, the relatively high signal intensity would suggest the presence of this deletion in a high number of cells in the population. With the additional weak signal of the FOXJ1 control, expected to show high knockout efficiency as shown in previous research (32), it is unclear whether it was really the CRISPR/Cas9 that caused the shift in sequence and thus a repeat of the experiment will provide more clarity. If higher efficiencies are not achieved, the use of Cas9-GFP and selection using FACS can be considered. Further investigation into this RNP knockout method is recommended because this procedure is less time consuming, and all materials can be easily commercially acquired for possibly a wide range of target genes and thus applications.

As shown, the tested lentiviral method has shown promising results in immortalized HNECs. The sequencing showed a sequence shift directly following the cutting site, indicating effective Cas9 activity potentially leading to CFTR knockout. Remarkably, despite positive selection with puromycin, there are also traces of the wildtype sequence in the bulk treated population. Therefore, for future applications, optimizations can be considered regarding the positive selection process. Based on the observed stress caused by puromycin, increasing the concentration would not be advised but the effect of puromycin selection at multiple time points during culturing can be investigated. Alternatively, replacing puromycin resistance with GFP expression for FACS-based selection of transduced cells, can be considered for many applications. Additionally, optimizations of positive selection and transduction efficiency can be considered to further investigate the possibility of transient expression with use of the non-integrating lentiviral particles. Possibly due to low density of puromycin resistant cells treated with these particles, the cells were not able to expand long after selection. That being said, for the main purpose of this research, it is crucial to know the exact number of CFTR-deficient cells, and thus the future focus will need to be on creating a clonal knockout line.

The ability to label both immortalized as primary cells with high efficiency, allows for more flexibility within the procedure to optimize the model. If higher representation of *in vivo* cells is a high priority with less of a need of long-term use, primary cells from a biobank can be preferred. This allows for a more personalized medicine approach for the diverse types of mutations with for example combinational use of CF-targeting drugs. However, for long term or preliminary proof-of-concept experiments, immortalized cells are ideal, as they do not have a limited proliferative capacity due to

continues expression of telomerase (TERT) (33). For example, insight into the gradual loss of mCherry signal or -positive cells was possible to discover due to the long-term expansion of these cells.

To further investigate the possibility of establishing the organoid model, mNeonGreen and mCherry immortalized cells were differentiated using the ALI procedure. As shown, the cells can be differentiated into secretory cells with functional CFTR and develop into mosaic organoids. During the first stage of the differentiation process, the seeded cells proliferate until full confluency. This means that differences in the initial green:red cell ratio can change during this stage. If at later stages deemed necessary, if for example more control of the final ratios is needed, this can be limited as much as possible by seeding a higher cell number to reach full confluency sooner. The final ratios in the mosaic organoids may also depend on variability in cell ratios within individual fragments of the monolayer that are converted into organoids. This depends on how evenly the cells are distributed across the ALI filters when seeded but also on the variability of the size of fragments when plated in Matrigel and how much more the cells will proliferate during organoid outgrowth. For these reasons, a variability of final cell ratios in organoids generated from one initial starting seeding ratio is expected.

With the use of computational segmentation, this variation can be mapped out by processing 3D confocal images to recognize and count every individual cell. To image and process a large number of organoids and correspond their counted green and red ratios with their FIS data, a lower magnification was decided on as preferred. This way higher throughput is possible while still being able to link cell ratios of individual organoids to FIS analysis data of the same organoids. Optimizations to achieve this goal were done to find the optimal settings at low magnification without losing the resolution required for proper segmentation. More is to be done in the future regarding pixel size and level of exposure of the cells within the organoids. A too high laser power and exposure time interferes with segmentation, but a too low exposure decreases visibility of cells in the lower z-positions of the organoids at 5x magnification. If this proves too much a problem, 10x magnification in combination of a higher organoid density or number of imaged wells, could provide a solution. Another observation from the optimization efforts, is that a higher number of slices in a z-stack could solve an observed issue of abnormally stretched out nuclei in the resulting 3D organoid images.

In the future, if the positive selection, imaging and segmentation hurdles are overcome, the goal is to generate mosaic organoids with immortalized or primary CFTR-proficient and CFTR-deficient cells, (knockout or patient-derived) for different types of *CFTR* mutations and gather enough data to get insight into the probability distribution of green and red cell ratios in cultured mosaic organoids. If then linked to their corresponding forskolin-induced swelling, an indication can be made of the number of CFTR-proficient cells required for sufficient functional recovery of CFTR-transport and consequently the efficiency of gene editing. When combined with drug testing for different *CFTR* variants, this model functions as a promising tool to progress towards an effective and targeted treatment for all CF patients.

References

1. Grasemann H, Ratjen F. Cystic Fibrosis. Taichman DB, editor. New England Journal of Medicine. 2023 Nov 2;389(18):1693–707.
2. Shteinberg M, Haq IJ, Polineni D, Davies JC. Cystic fibrosis. The Lancet. 2021 Jun 5;397(10290):2195–211.
3. Guo J, Garratt A, Hill A. Worldwide rates of diagnosis and effective treatment for cystic fibrosis. Journal of Cystic Fibrosis. 2022 May 1;21(3):456–62.
4. Plasschaert LW, MacDonald KD, Moffit JS. Current landscape of cystic fibrosis gene therapy. Front Pharmacol. 2024;15:1476331.
5. Wang G. Genome Editing for Cystic Fibrosis. Cells. 2023 Jun 1;12(12):1555.
6. Arjmand B, Larijani B, Sheikh Hosseini M, Payab M, Gilany K, Goodarzi P, et al. The horizon of gene therapy in modern medicine: Advances and challenges. Cell Biology and Translational Medicine. 2019;8:33–64.
7. Farmen SL, Karp PH, Ng P, Palmer DJ, Koehler DR, Hu J, et al. Gene transfer of CFTR to airway epithelia: Low levels of expression are sufficient to correct Cl- transport and overexpression can generate basolateral CFTR. Am J Physiol Lung Cell Mol Physiol. 2005 Dec;289(6):L1123–30.
8. Johnson LG, Olsen JC, Sarkadi B, Moore KL, Swanstrom R, Boucher RC. Efficiency of gene transfer for restoration of normal airway epithelial function in cystic fibrosis. Nat Genet. 1992;2:21–5.
9. Goldman MJ, Yang Y, Wilson JM. Gene therapy in a xenograft model of cystic fibrosis lung corrects chloride transport more effectively than the sodium defect. Nat Genet. 1995;9:126–31.
10. Zhang L, Button B, Gabriel SE, Burkett S, Yan Y, Skiadopoulos MH, et al. CFTR Delivery to 25% of Surface Epithelial Cells Restores Normal Rates of Mucus Transport to Human Cystic Fibrosis Airway Epithelium. PLoS Biol. 2009 Jul;7(7):e1000155.
11. Woodall M, Tarran R, Lee R, Anfishi H, Prins S, Counsell J, et al. Expression of gain-of-function CFTR in cystic fibrosis airway cells restores epithelial function better than wild-type or codon-optimized CFTR. Mol Ther Methods Clin Dev. 2023 Sep 14;30:593–605.
12. Shah VS, Ernst S, Tang XX, Karp PH, Parker CP, Ostedgaard LS, et al. Relationships among CFTR expression, HCO3- secretion, and host defense may inform gene- and cell-based cystic fibrosis therapies. Proc Natl Acad Sci U S A. 2016 May 10;113(19):5382–7.
13. Dannhoffer L, Blouquit-Laye S, Regnier A, Chinet T. Functional Properties of Mixed Cystic Fibrosis and Normal Bronchial Epithelial Cell Cultures. Am J Respir Cell Mol Biol. 2008 Dec 20;40(6).
14. Rafeeq MM, Murad HAS. Cystic fibrosis: current therapeutic targets and future approaches. J Transl Med. 2017 Apr 27;15(1):84.
15. Mall MA, Burgel PR, Castellani C, Davies JC, Salathe M, Taylor-Cousar JL. Cystic fibrosis. Nat Rev Dis Primers. 2024 Aug 8;10(53).
16. Silva S, Bicker J, Falcão A, Fortuna A. Air-liquid interface (ALI) impact on different respiratory cell cultures. European Journal of Pharmaceutics and Biopharmaceutics. 2023 Mar 1;184:62–82.
17. Rodenburg LW, van der Windt IS, Dreyer HHM, Smits SMA, den Hertog - Oosterhoff LA, Aarts EM, et al. Protocol for generating airway organoids from 2D air liquid interface-differentiated nasal epithelia for use in a functional CFTR assay. STAR Protoc [Internet]. 2023 Sep 15 [cited 2025 Feb 16];4(3). Available from: https://pmc.ncbi.nlm.nih.gov/articles/PMC10511861/
18. Hangjin L, Junting Y, Yiqin W, Hui Q, Shen Y, Jizhe W. Culture expansion of primary human nasal epithelial cells (NEC) isolated with a nasal scraping spoon. J Int Med Res. 2023 Nov 1;51(11).
19. Amatngalim GD, Rodenburg LW, Aalbers BL, Raeven HHM, Aarts EM, Sarhane D, et al. Measuring cystic fibrosis drug responses in organoids derived from 2D differentiated nasal epithelia. Life Sci Alliance. 2022 Dec 1;5(12):e202101320.

20. Rodenburg LW, van der Windt IS, Dreyer HHM, Smits SMA, den Hertog - Oosterhoff LA, Aarts EM, et al. Protocol for generating airway organoids from 2D air liquid interface-differentiated nasal epithelia for use in a functional CFTR assay. STAR Protoc. 2023 Sep 15;4(3):102337.
21. Boj SF, Vonk AM, Statia M, Su J, Vries RRG, Beekman JM, et al. Forskolin-induced Swelling in Intestinal Organoids: An In Vitro Assay for Assessing Drug Response in Cystic Fibrosis Patients. Journal of Visualized Experiments. 2017 Feb 11;(120):55159.
22. Dekkers JF, Berkers G, Kruisselbrink E, Vonk A, De Jonge HR, Janssens HM, et al. Characterizing responses to CFTR-modulating drugs using rectal organoids derived from subjects with cystic fibrosis. Sci Transl Med. 2016 Jun 22;8(344):344ra84.
23. Sanjana NE, Shalem O, Zhang F. Improved vectors and genome-wide libraries for CRISPR screening. Nat Methods. 2014;11(8):783–4.
24. Sanjana NE, Shalem O, Zhang F. Improved vectors and genome-wide libraries for CRISPR screening. Nat Methods. 2014;11(8):783–4.
25. Shalem O, Sanjana NE, Hartenian E, Shi X, Scott DA, Mikkelsen TS, et al. Genome-Scale CRISPR-Cas9 Knockout Screening in Human Cells. Science (1979). 2014;343:83–7.
26. New England Biolabs [Internet]. [cited 2025 Mar 5]. NEBcloner. Available from: https://nebcloner.neb.com/#!/
27. Kutner RH, Zhang XY, Reiser J. Production, concentration and titration of pseudotyped HIV-1-based lentiviral vectors. Nat Protoc. 2009 Mar 19;4:495–505.
28. Dull T, Zufferey R, Kelly M, Mandel RJ, Nguyen M, Trono D, et al. A third-generation lentivirus vector with a conditional packaging system. J Virol. 1998 Nov 1;72(11):8463–71.
29. Lefferts JW, Kroes S, Smith MB, Niemöller PJ, Nieuwenhuijze NDA, Sonneveld van Kooten HN, et al. OrgaSegment: deep-learning based organoid segmentation to quantify CFTR dependent fluid secretion. Commun Biol. 2024 Dec 1;7(1):319.
30. Smith MB, Li H, Shen T, Huang X, Yusuf E, Vavylonis D. Segmentation and Tracking of Cytoskeletal Filaments Using Open Active Contours. Cytoskeleton (Hoboken). 2010 Nov;67(11):693–705.
31. Smith MB, Chaigne A, Paluch EK. An active contour ImageJ plugin to monitor daughter cell size in 3D during cytokinesis. Methods Cell Biol. 2017 Jan 1;137:323–40.
32. Rapiteanu R, Karagyozova T, Zimmermann N, Wayne G, Martufi M, Belyaev NN, et al. Highly efficient genome editing in primary bronchial epithelial cells establishes FOXJ1 as essential for ciliation in human airways. European Respiratory Journal. 2020 Jan 31;55(5).
33. Shitova M, Alpeeva E, Vorotelyak E. Review of hTERT-Immortalized Cells: How to Assess Immortality and Confirm Identity. Int J Mol Sci. 2024 Dec 4;25(23):13054.